Supplementary Information for

Broadband ultrafast 2D NMR spectroscopy for online monitoring in continuous flow

Célia Lhoste, Margherita Bazzoni, Justine Bonnet, Aurélie Bernard, François-Xavier Felpin, Patrick Giraudeau, Jean-Nicolas Dumez*

Nantes Université, CNRS, CEISAM, UMR6230, F-44000 Nantes, France

Table of contents

1. Principles of interleaved acquisitions

In ultrafast 2D NMR, the acquisition block results in a zig-zag trajectory in the (k, t_2) space, where $k = \gamma \int G(t')dt'$ is the gradient area, as illustrated in Fig. S1. As a result, two consecutive time points with corresponding to the same k value are spaced by a dwell time of $2T_a$, leading to a conventional spectral width equivalent to:

$$SW_{conv} = \frac{1}{2T_a} \qquad (1)$$

Interleaved acquisitions consist of acquiring several consecutive scans for the same experiment, with a time shift τ of the start of the acquisition block for each scan.[1,2] As a result, each additional scan gives a shifted (k, t_2) trajectories. The case of 2 interleaved scans is illustrated in Fig. S1. The start of the second trajectory is shifted by $\tau = T_a$. When the two trajectories are combined, this effectively reduces the dwell time to T_a. This results in a doubled spectral width in the conventional dimension. This can be generalised to the acquisition of N interleaved scans, with time shifts of the form $\frac{n-1}{N}2T_a$, where n = 1, 2, … N.

Interleaved acquisitions make it possible to improve both spectral dimensions at the same time, by reducing the dwell time between two points to improve the conventional spectral widths and by increasing the acquisition gradient duration to improve the UF spectral width. Interleaved acquisitions require a high stability from one scan to the next, otherwise "ghost" images of the peak of interest appear in the spectrum.
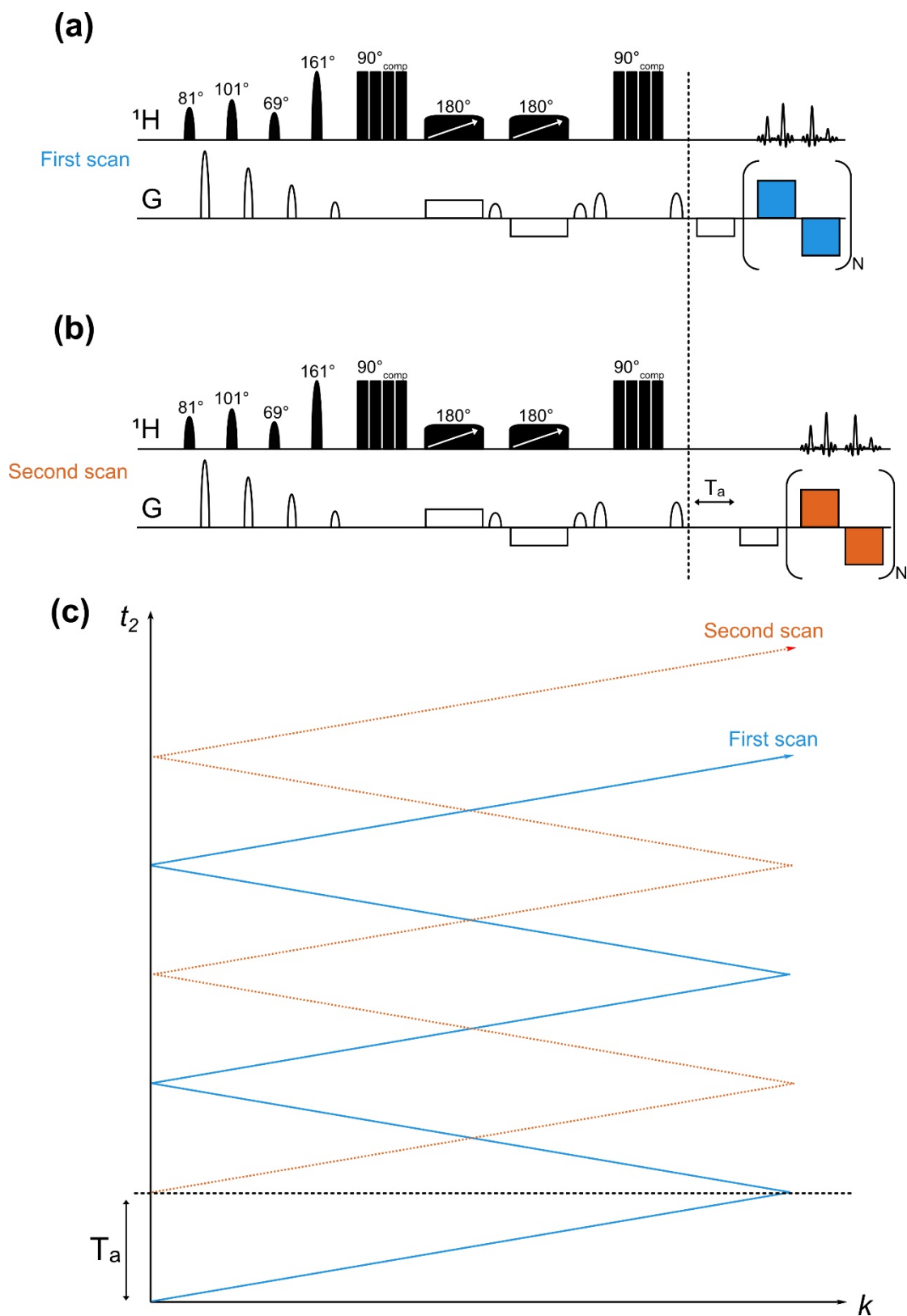
Fig. S1: Principle of interleaved scans. Pulse sequences for the first two scans are represented respectively in (a) and (b) to show the shifting of T_a between two interleaved scans. (c) Represents the different trajectories in the (k, t2) domain experienced in the two different scans.

2. Parameter optimisation

Procedure for parameters optimization

Sample. A solution of ethyl crotonate at a concentration of 0.22 M in MeOH or CHCl$_3$ was flown into the FlowNMR set-up.

As reference, two samples of ethyl crotonate at 0.22 M in MeOD and CDCl$_3$ were analysed with a conventional COSY pulse sequence (Bruker sequence cosygpmfppqf). The reference spectra are shown in Fig. S2. The number of signals is different between the conventional or the ultrafast COSY spectrum of ethyl crotonate due to the solvent which is deuterated in the case of the conventional experiment. As expected the resolution is better in the conventional experiment than in the ultrafast one.
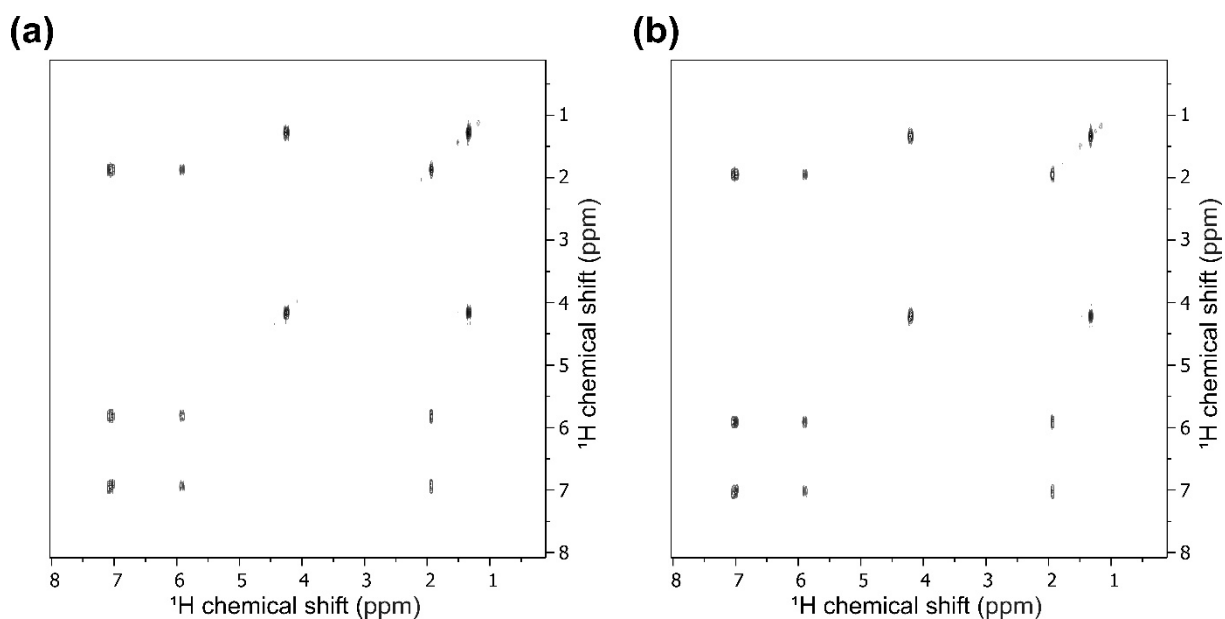

Fig. S2: (a) Reference conventional COSY spectra of ethyl crotonate at 0.22M (a) in CDCl$_3$ and (b) in MeOD, both acquired on a 400 MHz spectrometer.

In the following, the optimization of several parameters is described. Parameters were varied one by one, keeping the others to their default value given in section 1. The optimized parameters were the gradient axis for spatial encoding, the gradient axis for solvent suppression, the use or not of composite 90° pulses, the number of dummy scans, and the amplitude of coherence-selection gradients. Other parameters were explored such as the interleaving delay position, the gradient signs of the CSG around the second 90° pulse and the solvent suppression block between WET and WET180. These parameters did not have a noticeable impact and did not improve the quality of the spectrum.

Encoding axis*. The encoding axis optimization is described in the main text and in Fig. 3. Some extracted slices are described in the Fig. S3, to highlight the encoding axis and solvent impact on the ghost peaks.
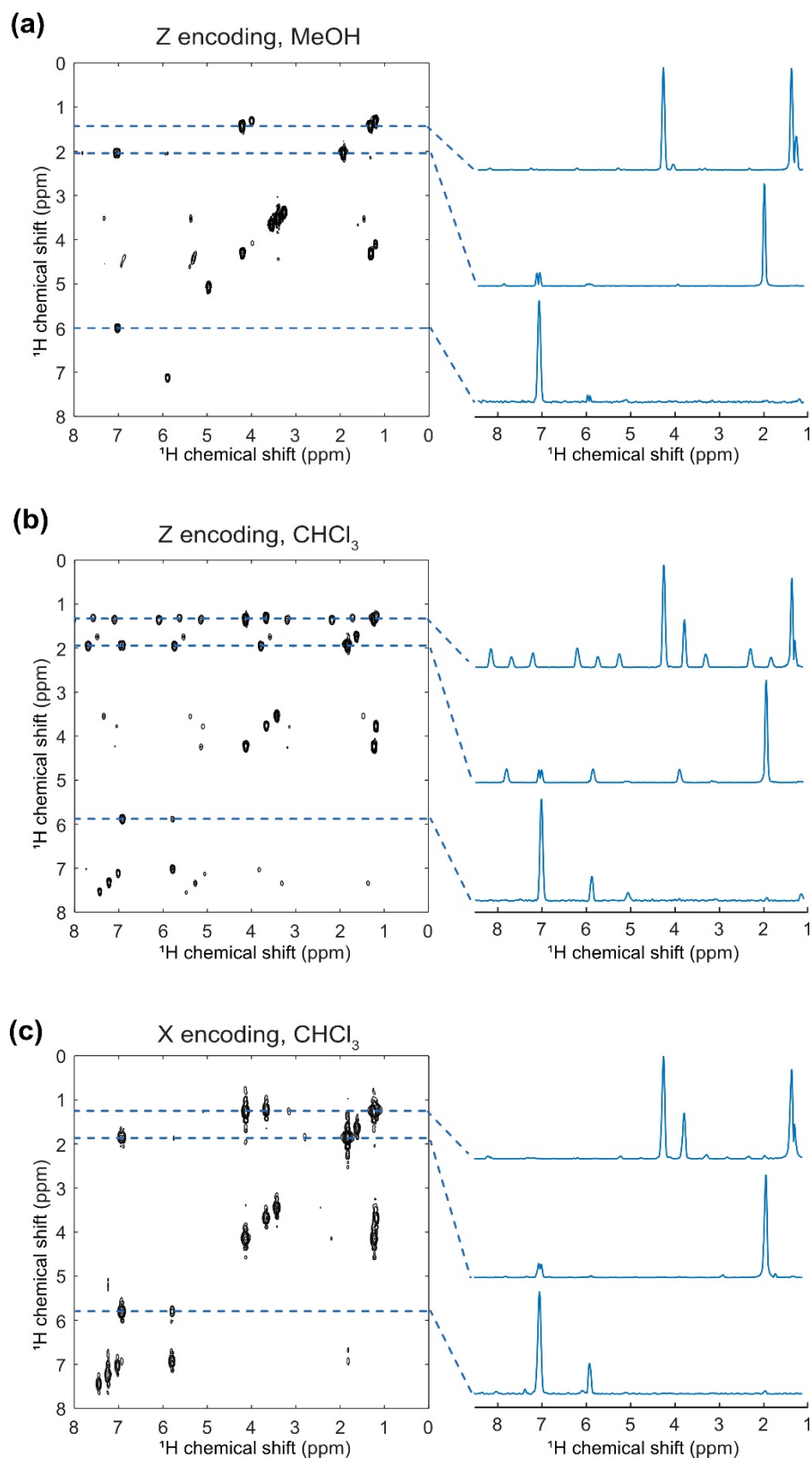

Fig. S3: Extracted-slices obtained from Fig. 3, for each slice, the intensity is normalized by the maximum signal intensity of the slice.

WET axis. The WET gradients axis optimization is described in the main text and in Fig. 4(a) and (b). Some extracted slices are described in the Fig. S4, to highlight the WET gradient axis impact on the ghost peaks and ghost stripes.
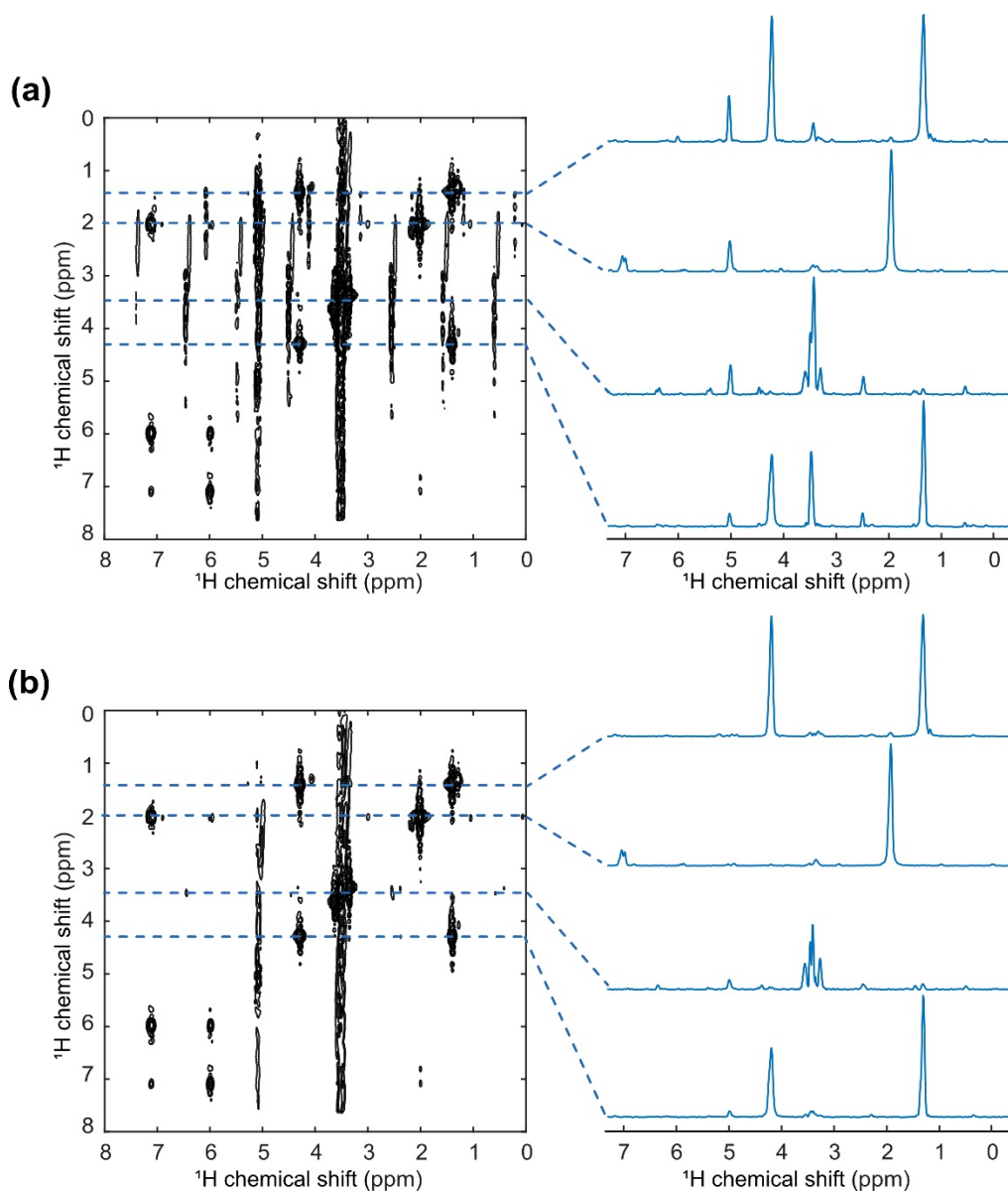

Fig. S4: Extracted-slices obtained from Fig. 2, for each pair of slices, the intensity is normalized by the maximum signal intensity between both slices (Same scale for comparable slices from different spectra, but not between slices of the same 2D spectrum). (a) WET gradients axis along X axis and (b) WET gradients axis along Z axis.

90° pulses. The comparison between regular and composite 90° pulses is described in the main text and in Fig. 4(c). The spectra used for the plotted peak volumes and error bars are described in the Fig. S5, to highlight the instability of the ghost stripes into the spectra. The comparison was done between the use of two 90° hard pulses (Fig. S5 (b)) and the use of two 90° composite pulses (Fig. S5 (a)). The impact of the composite pulse on the ghost stripes is not visible on the spectra due to the instability of the repetition mainly due to the flow. The aromatic correlations are more sensitive with composite pulses and allows to see the diagonal peak at 7 ppm, which is missing on the spectra without composite pulse. Solvent signals are more attenuated with composite pulses, it explains why these signals are really broader on the spectra acquired without composite pulse.
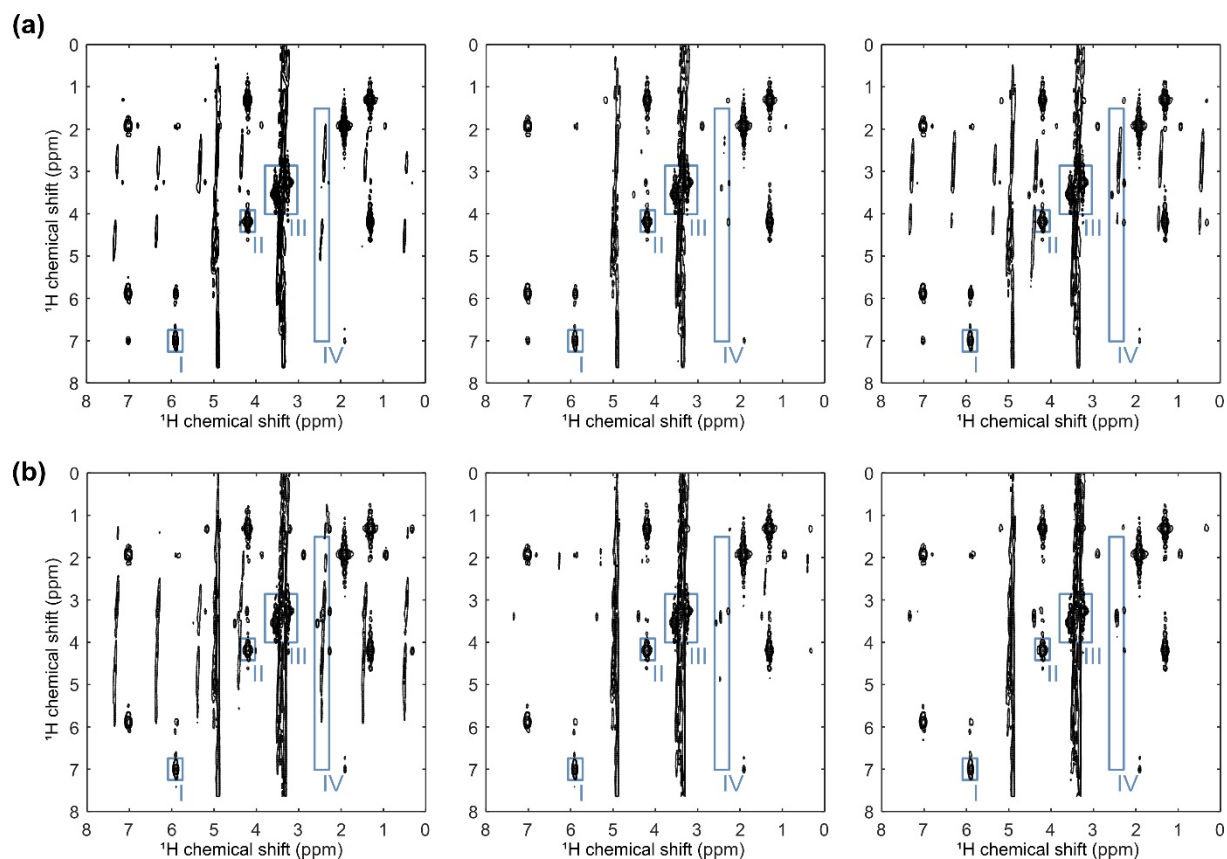
(a)

(b)

Fig. S5: 2D iUF COSY spectra comparison (a) with and (b) without composite pulses. Each line corresponds to 3 repetitions. All spectra were acquired with encoding axis along Y and WET solvent suppression gradients on Z axis. The flowrate is 1.5 mL/min. The sample is ethyl crotonate in MeOH at 0.22 M. The plotted peak volume represented in Fig. 4(c) in the main text are extracted from selected regions represented in blue on spectra, to compare signals obtained with and without composite pulses, for peaks of interest (cross (I) and diagonal (II) peaks), ghost stripe (IV) and solvent signal (III)).

Dummy scans. The number of dummy scans was varied to assess its effect on spectrum quality. The resulting peak volumes are described in Fig. S6. The use of one dummy scan shows a noticeable impact on the attenuation of the ghost peaks (i.e., images of the expected peaks). However, it did not attenuate the ghost stripe (i.e., images of the vertical stripes that are due to incomplete solvent suppression). Thus, one dummy scan was used for the reaction monitoring.
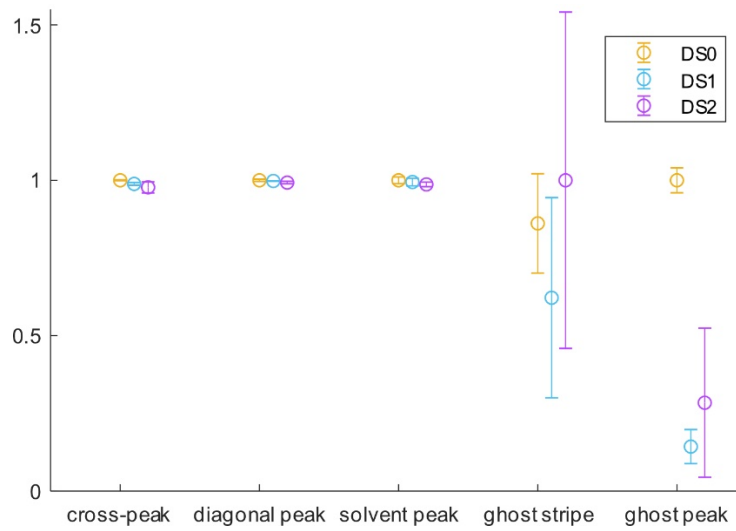
Fig. S6: Plotted peak volume extracted from selected region are represented to compare signals obtained with no, one or two dummy scan(s) for peaks of interest (cross and diagonal peaks), ghost peak and stripe and solvent signal. The peak volume regions are described in Fig. S7. The flowrate is 1 mL/min. All spectra were acquired with encoding axis along Y.
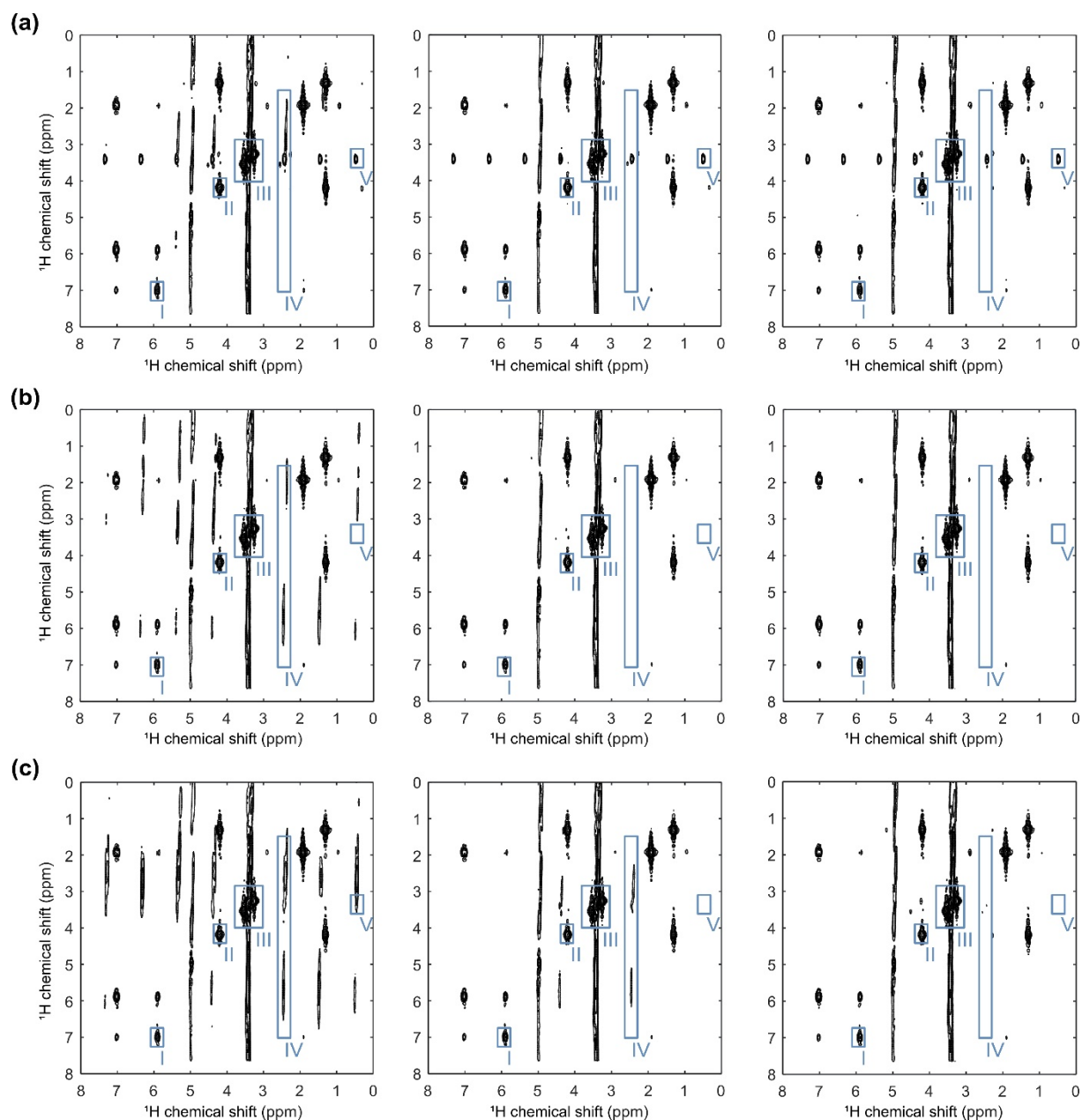
Fig. S7: 2D iUF COSY spectra comparison (a) with no dummy scan, (b) with one dummy scan and (c) with two dummy scans. Each line corresponds to 3 repetitions. All spectra were acquired with encoding axis along Y and WET solvent suppression gradients on Z axis. The flowrate is 1 mL/min. The sample is ethyl crotonate in MeOH at 0.22 M. The plotted peak volume represented in Fig. S6 are extracted from selected regions represented in blue on spectra, to compare signals obtained with 0, 1 or 2 dummy scan(s), for peaks of interest (cross (I) and diagonal (II) peaks), ghost peak (V) and ghost stripe (IV) and solvent signal (III)).

Coherence-selection gradients. The amplitude of the gradients around the second chirp pulse was tested between 0 and 44 G/cm as described in Fig. S8 and the amplitude of the gradients around the second 90° was tested between 0 and 44 G/cm as described in Fig. S9. Various flowrates were used such as 0 mL/min, 1.0 mL/min and 2.5 mL/min, to identify the impact of the flowrate on the quality of the spectra.

Fig. S8 shows that the attenuation of signals of interest and solvent signal is effective at an amplitude of the gradients around the second chirp pulse of minimum 10 G/cm. Even in static conditions, the

peak volume of the ghost stripe is not stable. A compromise needs to be done to limit the impact on the peaks of interest. An optimized value of around 10 G/cm has been choose for the reaction monitoring. The flow effect is also visible. Indeed, the ghost stripe volumes are more variable when the flow is on. Others signals have similar behaviors in both cases.
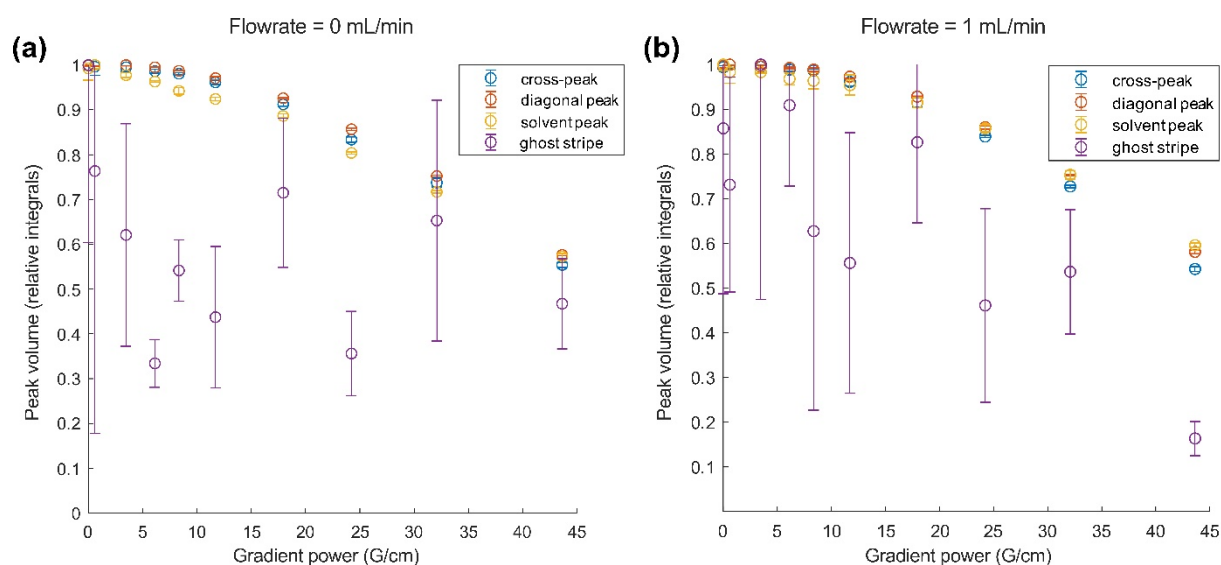

Fig. S8 Plotted peak volume extracted from selected region are represented to compare signals obtained for peaks of interest (cross (blue) and diagonal (orange) peaks), ghost stripe (purple) and solvent signal (yellow), with an array of amplitudes for gradients around the second chirp pulse. The peak volume regions are the same as in Fig. S5. The experiments were obtained in (a) static conditions and at (b) a flowrate of 1 mL/min. All spectra were acquired with encoding axis along Y.

Based on Fig. S9, the attenuation of solvent signal and anti-echo signal is effective at an amplitude of the gradients around the second 90° of minimum 10 G/cm. The intensities of the signals of interest are increase while the amplitude of the gradient increase. An optimized value of around 20 G/cm has been decided.
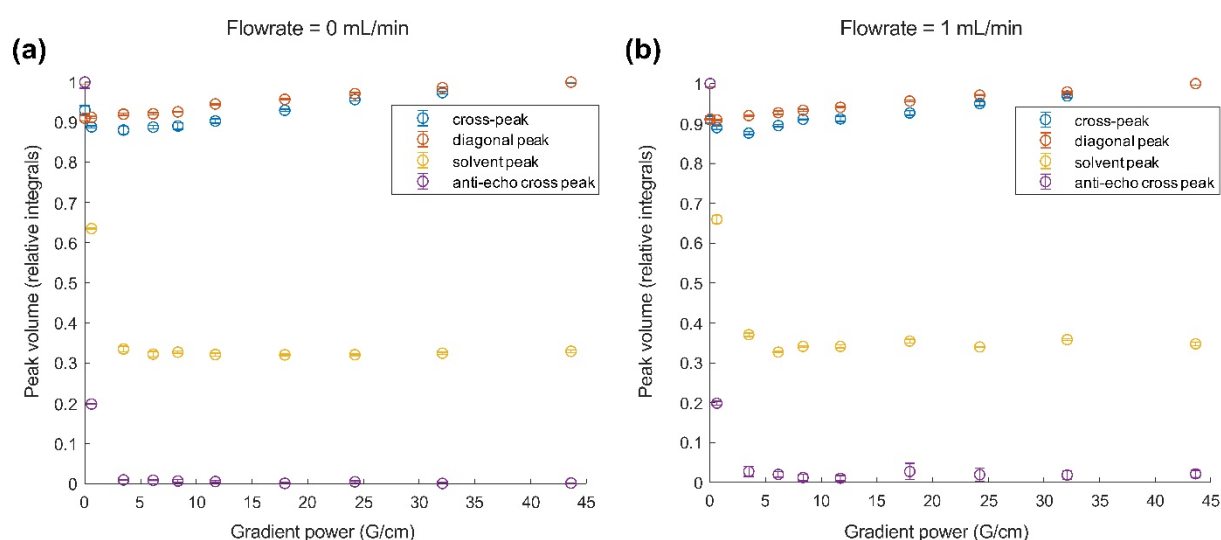

Fig. S9 Plotted peak volume extracted from selected region are represented to compare signals obtained for peaks of interest (cross (blue) and diagonal (orange) peaks), anti-echo cross peak (purple) and solvent signal (yellow), with an array of amplitudes for gradients around the second 90°. The peak volume regions are the same as in Fig. S5 except for the IV peak volume region which is replace by the

anti-echo cross peak of the I peak volume region. The experiments were obtained in (a) static conditions and at (b) a flowrate of 1 mL/min. All spectra were acquired with encoding axis along Y.
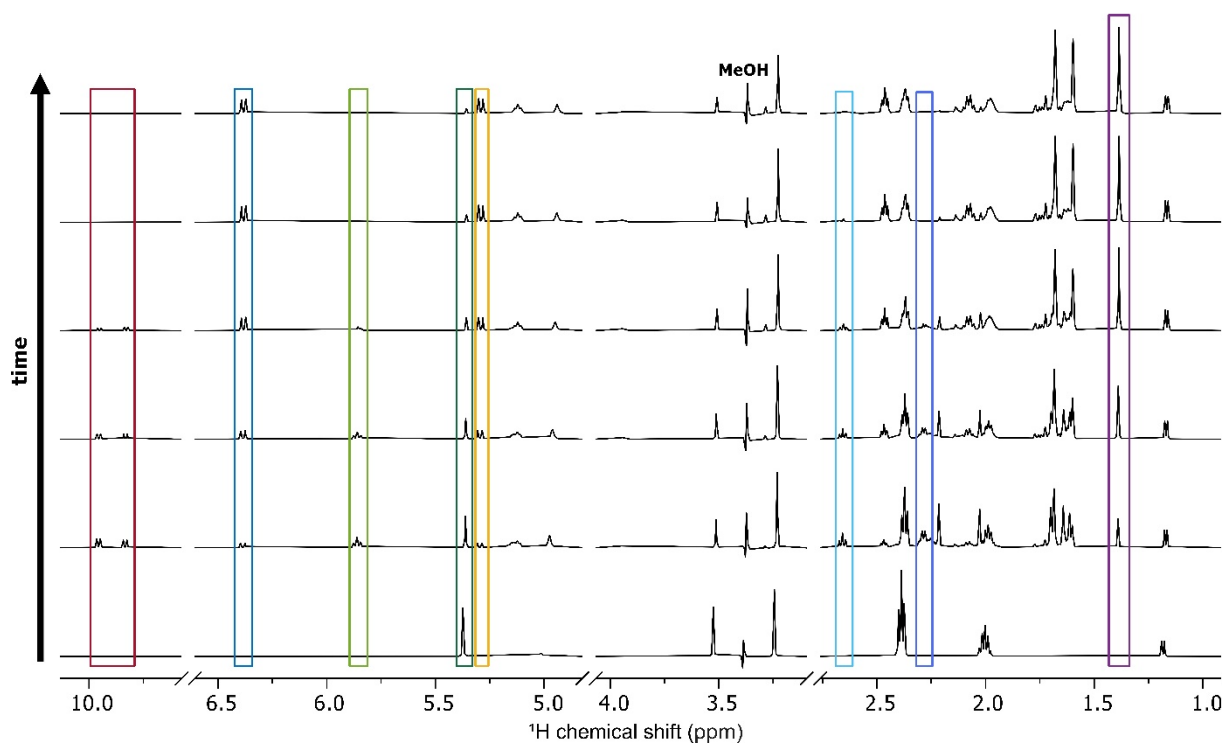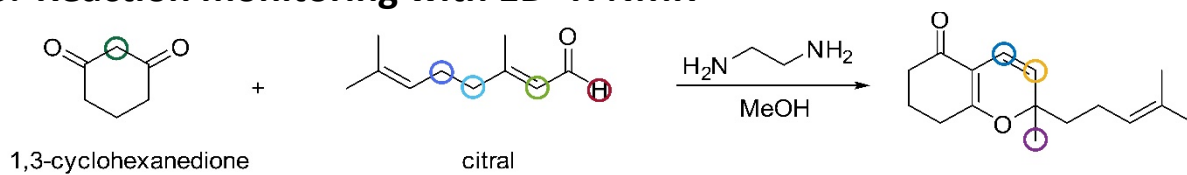
3. Reaction monitoring with 1D ^{1}H NMR

Fig. S10: 1D ^{1}H stacked spectra obtained during the reaction monitoring. The first spectrum (bottom) was obtained on the stabilised solution of 1,3-cyclohexanedione.
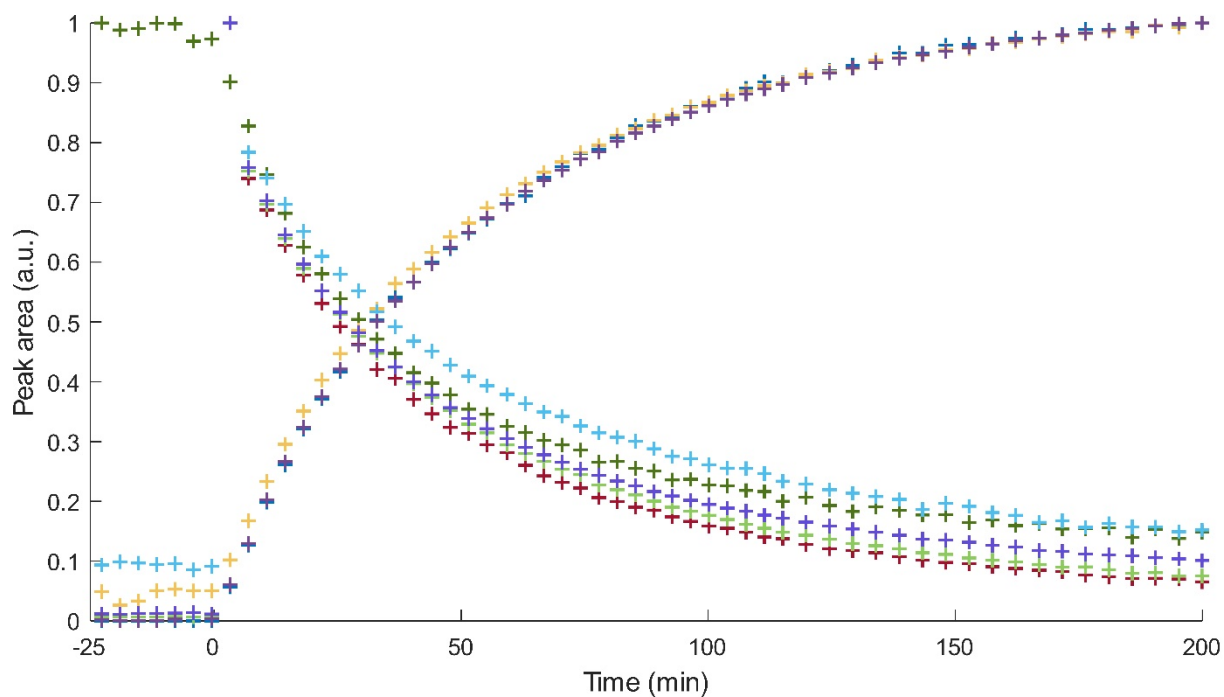
Fig. S11: 1D ^1H monitoring curves based on plotted peak area of some reagents and product correlations as a function of time. The flowrate was 1.5mL/min. Compared to Fig. 5 of the main text, the different behaviour of the cyclohexanedione peak volume can be explained by partial overlap with a product signal in the UF 2D spectrum.
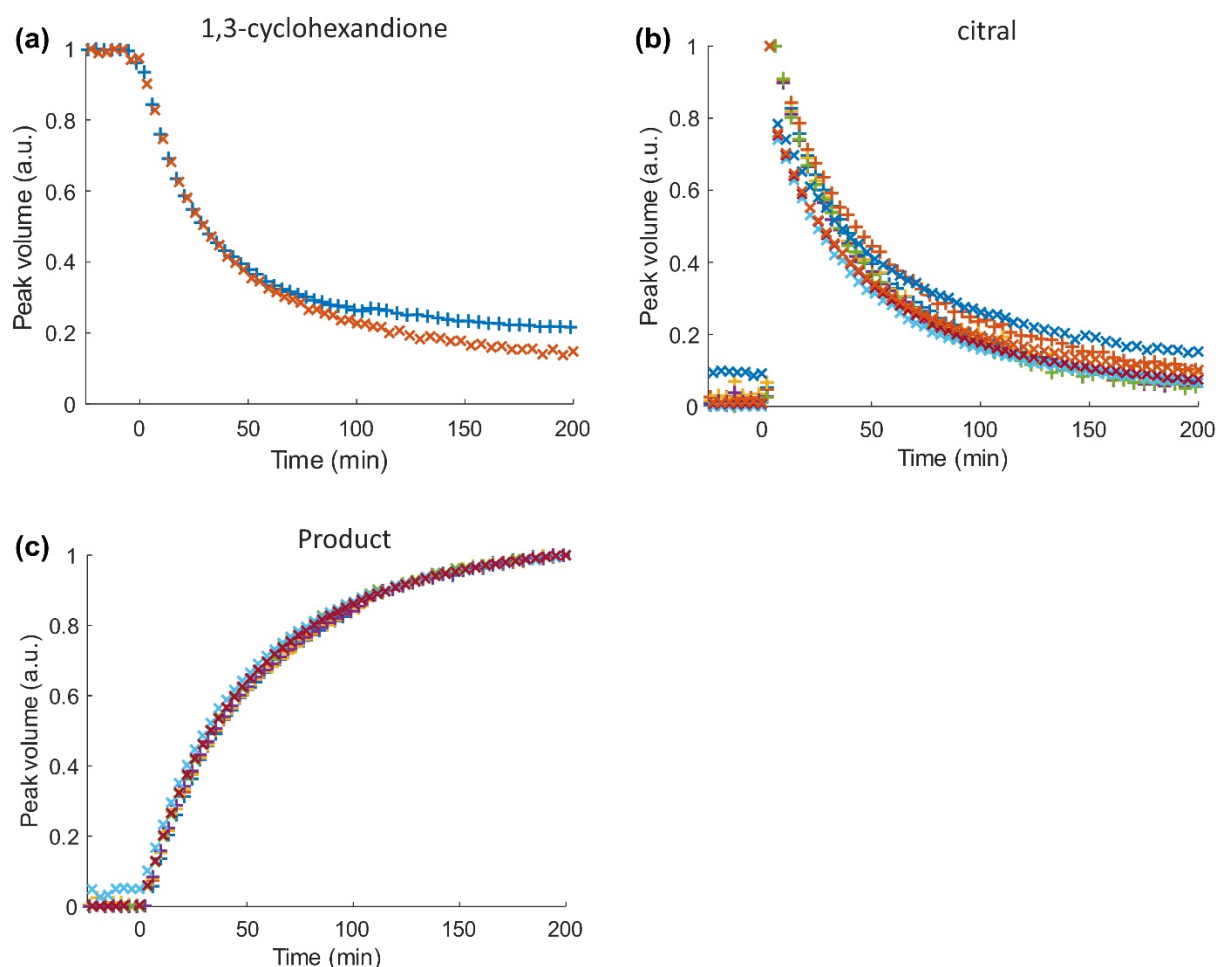
Fig. S12: 1D ^{1}H and UF 2D monitoring curves comparison, based on plotted peak area of some reagents and product correlations as a function of time. The crosses (x) correspond to the 1D ^{1}H data and the plus symbol (+) to the 2D UF data. The flowrate was 1.5mL/min.

4. Characterisation

2-methyl-2-(4-methylpent-3-en-1-yl)-2,6,7,8-tetrahydro-5H-chromen-5-one. An analytical sample was purified by flash chromatography on silica gel (5% AcOEt-cyclohexane). IR (ATR) *v* 2925, 1644, 1589, 1410, 1069 cm^{-1}. ^{1}H NMR (CDCl$_3$, 300 MHz) δ (ppm) 6.43 (d, 1H, *J* = 10.1 Hz), 5.16 (d, 1H, *J* = 10.1 Hz), 5.07 (ts, 1H, *J* = 1.4, 7.1 Hz), 2.38 (t, 2H, *J* = 6.8 Hz), 2.36 (t, 2H, *J* = 6.8 Hz), 1.91-2.08 (m, 4H), 1.50-1.72 (m, 2H), 1.65 (d, 3H, *J* = 1.0 Hz), 1.57 (br s, 3H), 1.35 (s, 3H). ^{13}C NMR (CDCl$_3$, 75 MHz) δ (ppm) 194.9, 172.1, 132.1, 123.8, 121.8, 116.5, 110.4, 82.4, 41.8, 36.5, 28.7, 27.5, 25.8, 22.6, 20.8, 17.7. HRMS (ASAP+) *m/z* [M + H]$^+$ Calcd for C$_{16}$H$_{23}$O$_2$ 247.1698; Found 247.1701.

5. Pulse sequence code for ultrafast COSY with WET block and composite pulses

;This pulse program has been created by Célia Lhoste and Margherita Bazzoni, based on an initial pulse program by Patrick Giraudeau and Serge Akoka, CEISAM, Nantes Université, France
;The authors are not responsible for the results obtained with this pulse sequence, and decline responsibility for any damage resulting from the use of this program
;Please do not delete this header from the pulse program.

;$CLASS=HighRes
;$DIM=2D
;$TYPE=
;$SUBTYPE=
;$COMMENT=

prosol relations=<lcnmr>

#include <Avance.incl>
#include <Grad.incl>
#include <De.incl>
#include <Delay.incl>

define delay WETWAIT

"d0=3u"
"d11=30m"
"d20=(td*dw/(2*l3))-d6"
"p24=d20"
"d2=3u"
"in2=2*(d20+d6)/td1"

"d12=20u"
"d13=4u"
"d16=2m"

"WETWAIT=2.5m-d16"

"acqt0=-(p1*6/3.1416)-4u"

"d25=1u*abs(cnst25)" ;just to display cnst25
"d23=1u*abs(cnst3)";just to display cnst3

1 ze

```
2 30m
        10u ;reset:f1:f2
        4u ;cw:f2 ph29
  d1
        4u ;do:f2
  100u UNBLKGRAD


;--------------- solvent suppression block (WET)


        d12 pl0:f1
  d13
  (p12:sp7 ph5):f1
  4u
  p16:gp11
  d16 pl0:f1
  (p12:sp8 ph6):f1
  4u
  p16:gp12
  d16 pl0:f1
  (p12:sp9 ph6):f1
  4u
  p16:gp13
  d16 pl0:f1
  (p12:sp10 ph6):f1
  4u
  p16:gp14
  d16
  WETWAIT pl1:f1


;--------------- excitation with spatially slective composite pulse


  p1 ph1
  4u
  p1 ph2
  4u
  p1 ph3
  4u
  p1 ph4


  d10


;--------------- spatial encoding step
  d4 gron0
  p11:sp1:f1 ph1
  d4 groff
  p20:gp20
  d4 gron1
  p11:sp1:f1 ph2
```

```
  d4 groff
  p21:gp21


;-------------- pre-mixing gradient
  d4
       p24:gp24
  d4


;-------------- mixing
  p23:gp23
  d4
  5u pl1:f1

  p1 ph1
  4u
  p1 ph2
  4u
  p1 ph3
  4u
  p1 ph4

  d4
  p26:gp26
          d2


;-------------- post-mixing gradient
  d4
  d20 gron2*cnst25
  d6 groff


;-------------- acquisition
  ACQ_START(ph30,ph31)
  1u DWELL_GEN:f1
3 d20 gron2
  d6 groff
  d20 gron2*cnst3
  d6 groff
  lo to 3 times l3
          100u BLKGRAD
  rcyc=2
  100u UNBLKGRAD
  p27:gp27
  100u BLKGRAD
  30m mc #0 to 2 F1QF(id2)
  d17
          d25
          d23
exit
```

ph1=1
ph2=2
ph3=3
ph4=0
ph5=0
ph6=1
ph29=0
ph30=0
ph31=0

;pl0 : 0W
;pl1 : f1 channel - power level for pulse (default)
;sp1: shaped pulse power level for selective detection
;sp7: f1 channel - shaped pulse
;sp8: f1 channel - shaped pulse
;sp9: f1 channel - shaped pulse
;sp10: f1 channel - shaped pulse
;p1 : f1 channel - 90 degree high power pulse
;p11: f1 channel - 180 degree selective pulse (example : Chirp pulse)
;p12: f1 channel - 90 degree shaped pulse for solvent suppression
;p16: homospoil/gradient pulse   [2msec]
;p23 : coherence-selection gradient for mixing (p23=p26) [1000us]
;p26 : coherence-selection gradient for mixing (p23=p26) [1000us]
;p20 : coherence-selection gradient for spatial encoding (p20=p21) [800-1200us]
;p21 : coherence-selection gradient for spatial encoding (p20=p21) [800-1200us]
;spnam1 : shaped pulse for selective detection
;d1 : relaxation delay; 1-5 * T1 [minimum 5s if several scans or ds>0 or interleaving]
;d4 : gron/groff delay
;d11: delay for disk I/O   [30msec]
;d12: delay for power switching   [20 usec]
;d13: short delay   [4 usec]
;d16: delay for homospoil/gradient recovery
;d20 + d6 : acquisition gradient duration
;d17 : delay after experiment (delay to rest after long acquisition - 20 min)
;ns : 1 (or more if necessary)
;l3 : Number of loops for acquisition
;cnst3: factor to correct the difference between positive and negative gradients [-1 for no correction], to equilibrate gradients
;cnst25: factor for the prephasing gradient

;Gradient strength :
;gpz0 : strength for excitation gradient [0-100] (to calibrate with the chirp - usually 2-3 %)
;gpz1 : strength for reversed excitation gradient GPZ1 = -GPZ0
;gpz2 : strength for acquisition gradient
;gpz11 : 80%
;gpz12 : 40%
;gpz13 : 20%

;gpz14 : 10%
;gpz20 : coherence-selection gradient for spatial encoding (GPZ20=GPZ21) [80]
;gpz21 : coherence-selection gradient for spatial encoding (GPZ20=GPZ21) [80]
;gpz23 : coherence-selection gradient for mixing (GPZ26=+/-GPZ23) [80]
;gpz26 : coherence-selection gradient for mixing (GPZ26=+/-GPZ23) [+/-80]
;gpz24 : pre-mixing gradient - for folding
;gpz25: post-mixing gradient - for folding

;Use gradient files :
;gpnam20 : SINE.100
;gpnam21 : SINE.100
;gpnam23 : SINE.100
;gpnam26 : SINE.100
;gpnam24 : SMSQ10.32
;gpnam25 : SMSQ10.32

;IMPORTANT :
;   AQ max = 100 ms
;   d1 minimum = 5s if several scans or ds>0 or interleaving
;   maximum 20 min of UF in a row, then leave 20 min rest (d17) before performing UF
again
;   d20+d6 >= 200 us so d20 >= 180µs

;use TD1 for interleaving

6. References

1 L. Frydman, A. Lupulescu and T. Scherf, *J. Am. Chem. Soc.*, 2003, **125**, 9204–9217.

2 C. Lhoste, B. Lorandel, C. Praud, A. Marchand, R. Mishra, A. Dey, A. Bernard, J.-N. Dumez and P. Giraudeau, *Prog. Nucl. Magn. Reson. Spectrosc.*, 2022, **130–131**, 1–44.